Synthesis and Characterization of π-Extended Triangulene

Shantanu Mishra[†,⊥], Doreen Beyer[‡,⊥], Kristjan Eimre[†], Junzhi Liu[‡], Reinhard Berger[‡], Oliver Gröning[†], Carlo A. Pignedoli[†], Klaus Müllen[∥], Roman Fasel[†,§], Xinliang Feng[‡,*] and Pascal Ruffieux[†,*]

[†]nanotech@surfaces Laboratory, Empa – Swiss Federal Laboratories for Materials Science and Technology, Dübendorf, Switzerland

[‡]Faculty of Chemistry and Food Chemistry, and Center for Advancing Electronics Dresden, Technical University of Dresden, Dresden, Germany

[∥]Department of Synthetic Chemistry, Max Planck Institute for Polymer Research, Mainz, Germany

[§]Department of Chemistry and Biochemistry, University of Bern, Bern, Switzerland

Supporting Information Placeholder

ABSTRACT: The electronic and magnetic properties of nanographenes strongly depend on their size, shape and topology. While many nanographenes present a closed-shell electronic structure, certain molecular topologies may lead to an open-shell structure. Triangular-shaped nanographenes with zigzag edges, which exist as neutral radicals, are of considerable interest both in fundamental science and for future technologies aimed at harnessing their intrinsic high-spin magnetic ground states for spin-based operations and information storage. Their synthesis, however, is extremely challenging owing to the presence of unpaired electrons, which confers them with enhanced reactivity. We report a combined in-solution and on-surface synthesis of π-extended triangulene, a non-Kekulé nanographene with the structural formula $C_{33}H_{15}$, consisting of ten benzene rings fused in a triangular fashion. The distinctive topology of the molecule entails the presence of three unpaired electrons that couple to form a spin quartet ground state. The structure of individual molecules adsorbed on an inert gold surface is confirmed through ultra-high-resolution scanning tunneling microscopy. The electronic properties are studied *via* scanning tunneling spectroscopy, wherein unambiguous spectroscopic signatures of the spin-split singly-occupied molecular orbitals are found. Detailed insight into its properties is obtained through tight-binding, density functional and many-body perturbation theory calculations, with the latter providing evidence that π-extended triangulene retains its open-shell quartet ground state on the surface. Our work provides unprecedented access to open-shell nanographenes with high-spin ground states, potentially useful in carbon-based spintronics.

The synthetic chemistry of polycyclic conjugated hydrocarbons, or nanographenes (NGs), has witnessed a resurgent interest since the isolation of graphene.[1] The impetus for this development comes from the critical dependence of the physico-chemical properties of NGs on molecular size and shape, and more drastically, on molecular topology.[2–4] This renders the field of NGs a fertile playground to investigate rich structure-property relationships and emergent phenomena in purely organic materials. While many of the NGs realized to date exhibit a non-magnetic, closed-shell electronic structure, some NGs, as a result of their peculiar topology, may exhibit a magnetic, open-shell structure.[5] Such compounds are highly attractive for applications in molecular electronics,[6,7] non-linear optics[8] and photovoltaics.[9] Furthermore, unpaired spins in open-shell NGs may be used to perform spin logic operations for future spintronic applications.[10,11] In this respect, the family of NGs with triangular topology (see Chart 1) has received widespread attention as high-spin organic ferromagnets.[12] The unique topology of these compounds implies that no Kekulé valence structures can be drawn without leaving unpaired electrons.[13] The underlying physical basis for the non-Kekulé structure of these compounds is an inherent sublattice imbalance in the bipartite honeycomb lattice, such that not all p_z electrons can be paired to form π-bonds, which thus generates uncompensated radicals.[14,15] The effect of molecular topology on the magnetic ground state may be quantified using Ovchinnikov's rule,[16] which states that for alternant NGs, the ground state spin quantum number $S = (N_A\text{-}N_B)/2$; where N_A and N_B refer to the number of carbon atoms belonging to the two interpenetrating sublattices of the honeycomb lattice. As shown in Chart 1, this rule predicts increasing total spin with the increasing size of triangular NGs. Derivatives of phenalenyl (three fused benzene rings)[17] and triangulene (six fused benzene rings)[18–20] have been obtained in solution, and generation of unsubstituted triangulene was only recently reported *via* scanning tunneling microscopy (STM)-based atomic manipulation route.[21] However, larger homologues of the series with higher spin ground states remain elusive. The presence

Chart 1. Non-Kekulé NGs with triangular topology[a]

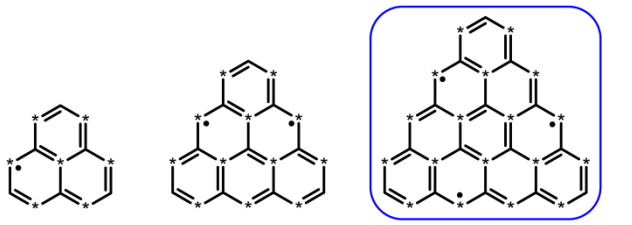

[a]*N** and *N* denote the number of atoms belonging to *A* and *B* sublattices, respectively. *S* denotes the total spin quantum number derived from Ovchinnikov's rule.[16]

Scheme 1. Synthetic route toward π-extended triangulene[b]

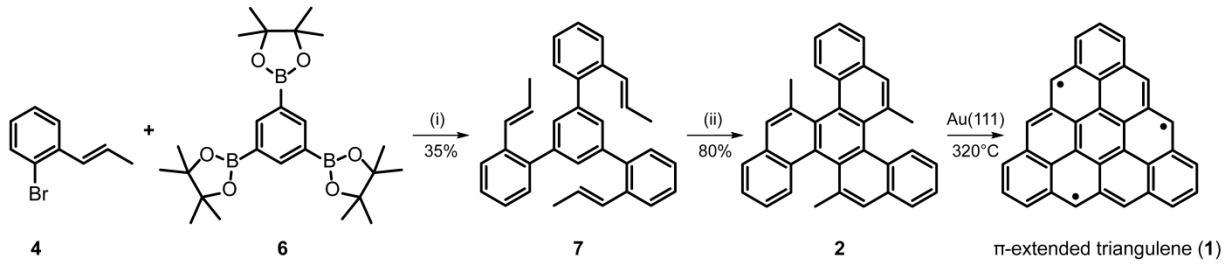

[b]Reagents and conditions: (i) K_2CO_3, $Pd(PPh_3)_4$, toluene/EtOH/H_2O, 110 °C, 18 h; and (ii) I_2, MCH, PPO, hν (λ = 253 nm), 8 h.

of unpaired electrons makes a conventional solution-based synthesis of such compounds extremely challenging,[22] and in this regard, on-surface synthesis under ultra-high vacuum conditions is a powerful alternative approach to achieve highly reactive compounds.[23] In addition to its potential toward large-scale generation of individual molecules, on-surface synthesis also holds great promise in the fabrication of extended nanostructures *via* appropriate design and functionalization of precursor molecules. Herein, we report a combined in-solution and on-surface synthesis of π-extended triangulene (**1**), consisting of ten fused benzene rings with three unpaired electrons. STM measurements evidence the chemical structure of **1**, and we unravel the electronic structure through scanning tunneling spectroscopy (STS), which clearly reveals the spin splitting of frontier orbitals. Our results are further supported by tight-binding and *ab-initio* calculations, which provide detailed insight into the electronic structure of this elusive compound.

The synthesis of **1** is based on precursor **2** (Scheme 1), consisting of a benzo[*c*]naphtho[2,1-*p*]chrysene core with three strategically-placed methyl substituents which serve as active sites that undergo oxidative ring closure reactions when **2** is annealed on a metal surface, leading to the formation of **1**. For the synthesis of **2**, it was expected that the photoactive key intermediate **7** should provide **2** *via* solution-mediated oxidative photocyclization. The synthetic approach to obtain **7** requires a three-step procedure (see Supplementary Information for detailed synthetic methodology) starting from the commercially available compounds 2-bromobenzaldehyde (**3**) and 1,3,5-tribromobenzene (**5**). Firstly, the quantitative, stereoselective synthesis of (*E*)-1-bromo-2-(prop-1-enyl)benzene (**4**) was carried out from **3** in the presence of pentan-3-one and boron trifluoride diethyl etherate (BF_3OEt_2), according to literature protocol.[24,25] Then, a Miyaura borylation reaction of 1,3,5-tribromobenzene (**5**) affords 1,3,5-phenyltriboronic acid trispinacol ester (**6**) in 52% yield.[26] Thereafter, the Suzuki cross-coupling reaction between **4** and **6** affords **7** in 35% yield. Finally, **7** was subjected to a photocyclization reaction under an inert atmosphere in the presence of methylcyclohexane (MCH), (±)propylene oxide (PPO) and iodine (I_2). Synthesis optimization revealed that a wavelength of 253 nm is most suitable to enforce conversion of **7** into **2**, in 80% yield.

Subsequently, a submonolayer coverage of **2** was deposited on Au(111) surface held at room temperature and annealed to 320 °C to promote surface-catalyzed ring closure reactions. Figure 1a presents an overview STM image of the surface after the annealing process, wherein the presence of individual molecules and irregular covalently-bonded molecular clusters can be discerned. Approximately 17% of the molecules present on the surface exhibit a uniform three-fold symmetric appearance (highlighted in Fig. 1a, also see Fig S1). High-resolution STM imaging of an individual molecule (Fig. 1b) reveals distinct electronic contrast in the local density of states (LDOS) as two prominent lobes at the three vertices and two weaker lobes along the edges of the molecule. To access the chemical structure of the molecule, we performed ultra-high-resolution STM imaging with a carbon monoxide (CO)-functionalized tip in the regime of tip-molecule Pauli repulsion,[27–29] which confirms the successful formation of **1** (Fig. 1c, also see Fig. S2 for height-dependent imaging data). The stable and planar adsorption of **1** on Au(111) as seen from STM imaging indicates the absence of any chemical bonding to the surface, and is in line with density functional theory (DFT) calculations (Fig. 1d) which reveal a flat adsorption geometry of **1** on gold, with the zigzag edges of **1** oriented along the nearest-neighbor gold atomic rows.

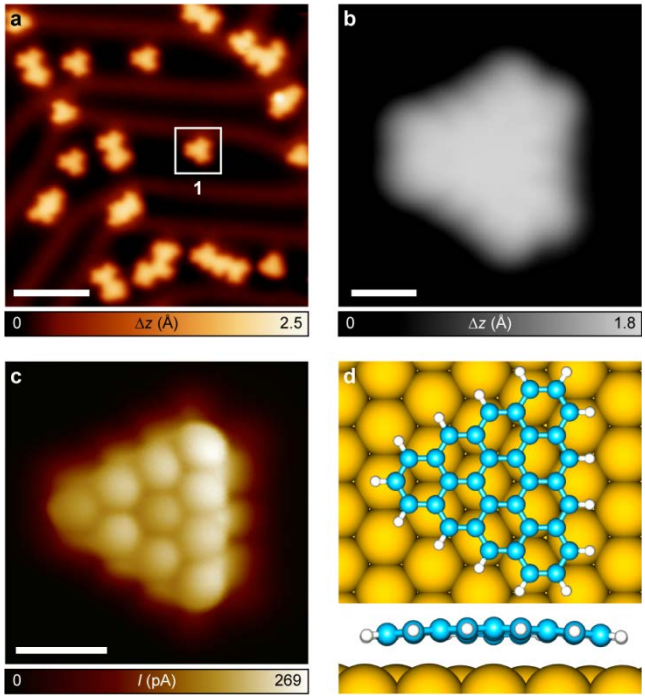

Figure 1. On-surface synthesis and structural characterization of π-extended triangulene on Au(111). (a) Overview STM topography image after annealing precursor **2** on Au(111) at 320 °C, revealing the predominant presence of individual three-fold symmetric molecules (one such molecule is highlighted with a white square) and fused molecular clusters (V = -600 mV, I = 60 pA). (b) High-resolution STM image of **1** acquired with a CO-functionalized tip (V = -400 mV, I = 100 pA). (c) Corresponding ultra-high-resolution STM image (V = -5 mV, I = 50 pA, Δz = -0.8 Å). (d) Top and side views of the DFT-optimized equilibrium geometry of **1** on Au(111). Scale bars: 5 nm (a) and 0.5 nm (b, c).

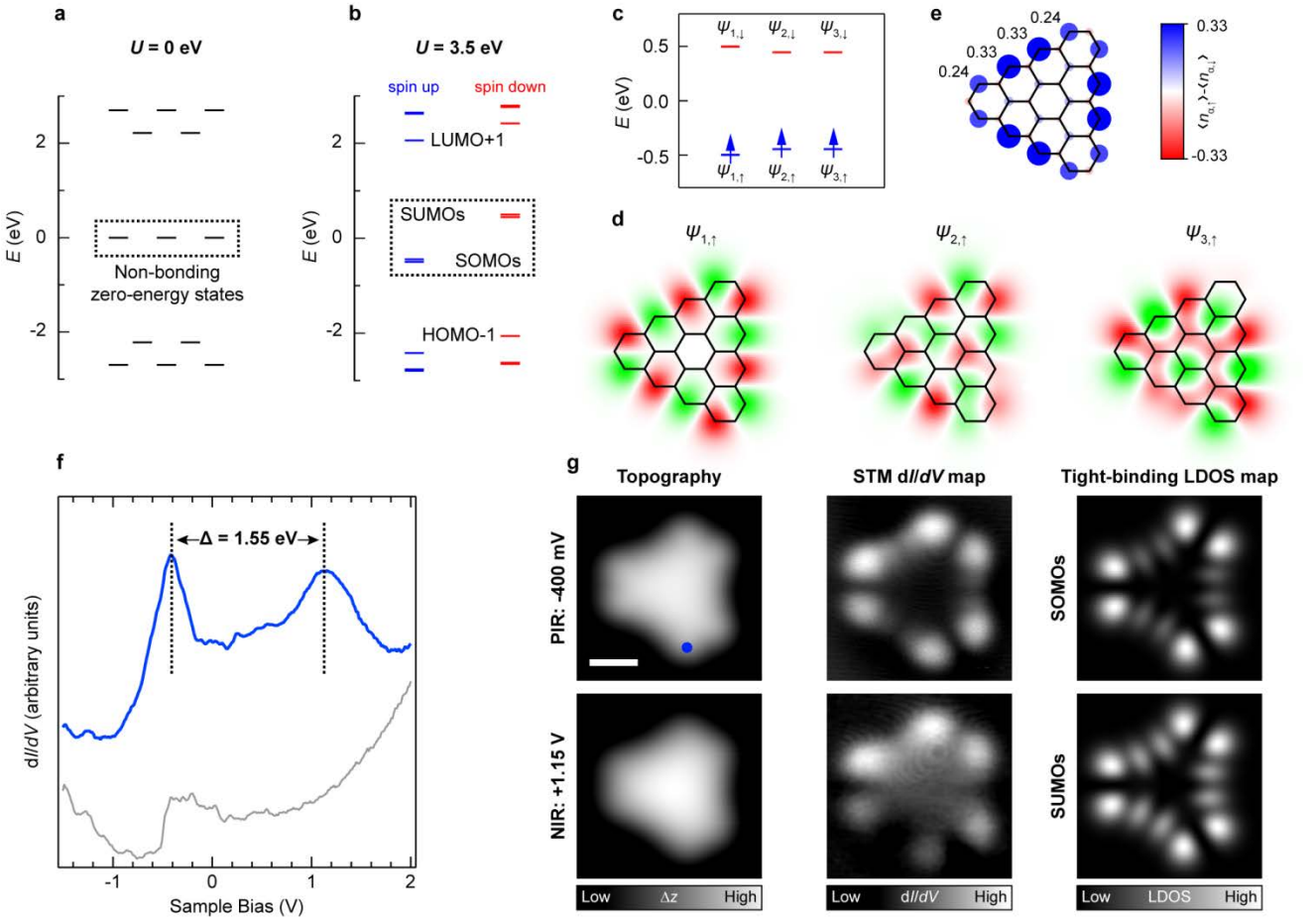

Figure 2. Electronic characterization of π-extended triangulene. (a, b) Nearest-neighbor TB (a) and MFH spectrum (b) of **1** showing three non-bonding zero-energy states and subsequent opening of a gap due to spin polarization. *U* denotes the on-site Coulomb repulsion. (c) Energy level scheme of the spin-polarized frontier orbitals ψ_1, ψ_2 and ψ_3 of **1**. (d) Computed wavefunctions of the SOMOs. Green/red isosurfaces denote opposite phase of the wavefunction. (e) Computed spin density distribution of **1**. Blue/red isosurfaces denote spin up/spin down density. Numbers denote spin density values. (f) d*I*/*dV* spectrum acquired on **1** (blue curve) at the position marked with a blue circle in (g). Gray curve corresponds to reference spectrum acquired on Au(111) (V = -1.5 V, I = 450 pA, V_{rms} = 12 mV). The spectra are vertically offset for visual clarity. (g) Constant-current STM images (left panels) and simultaneously acquired d*I*/*dV* maps at bias values corresponding to the PIR and NIR (center panels), along with simulated TB-LDOS maps of SOMOs and SUMOs of **1** (right panels). Tunneling parameters for the STM images and associated d*I*/*dV* maps: V = -400 mV, I = 400 pA (PIR) and V = +1.15 V, I = 420 pA (NIR); V_{rms} = 22 mV. Scale bar: 0.5 nm.

The electronic structure of **1** can be described well within the nearest-neighbor tight-binding (TB) model. The most important feature in the TB energy spectrum of **1** is the presence of three non-bonding, half-filled zero-energy states (Fig. 2a). Inclusion of electron correlation within the mean-field Hubbard (MFH) model induces spin polarization in the system, and leads to the opening of a Coulomb gap (Fig. 2b). The energy level scheme of the frontier orbitals is presented in Fig. 2c, which shows three quasi-degenerate singly-occupied molecular orbitals (SOMOs), with the populating spins aligned parallel to each other to give rise to an open-shell quartet (*i.e.* spin-3/2) ground state. The magnetic structure of **1** computed *via* MFH calculations is in agreement with previous theoretical reports[30] and our spin-polarized DFT calculations, where we also find the open-shell quartet state as the ground state, with the open-shell doublet (*i.e.* spin-1/2) state 236 meV higher in energy. The computed spin-polarized wavefunctions of the SOMOs are displayed in Fig. 2d, which exhibit a dominant edge-localized character with maximum amplitude on one sublattice only. Similarly, the computed spin density distribution shown in Fig. 2e reveals spin localization mostly at the zig-zag carbon atoms of sublattice *A* with negligible spin density on the atoms of sublattice *B*.

The principal outcomes of TB analyses are reproduced in our STS experiments, wherein d*I*/*dV* spectroscopy on **1** reveals broad and pronounced peaks in the DOS centered at -400 mV and +1.15 V (Fig. 2f, also see Fig. S3 for additional STS measurements), which correspond to the positive and negative ion resonances (PIR and NIR), respectively. Spatial mapping of the d*I*/*dV* signal (d*I*/*dV* maps) at these bias values (Fig. 2g) exhibits excellent correspondence to the TB-LDOS maps of the SOMOs (-400 mV) and the singly-unoccupied molecular orbitals (SUMOs, +1.15 V) of **1**. This confirms the assignment of the peaks in the d*I*/*dV* spectrum to molecular orbital resonances, and the associated Coulomb gap of **1** is deduced to be 1.55 eV. To determine the magnetic ground state of **1** adsorbed on Au(111), we performed eigenvalue self-consistent GW calculations including image charge screening effects from the underlying surface (GW+IC calculations, see Fig. S4) for the open-shell quartet and doublet electronic configurations. From these calculations, it is found that the experimental

Coulomb gap of 1.55 eV shows excellent agreement to the GW+IC frontier orbital gap of 1.67 eV of the open-shell quartet state of **1**, while the GW+IC frontier orbital gap of 640 meV of the open-shell doublet state differs significantly from the experimental value. These observations thus strongly suggest that **1** exhibits an open-shell quartet ground state on Au(111).

In summary, we have synthesized stable and unsubstituted π-extended triangulene adsorbed on a gold surface. Our synthetic protocol combines in-solution synthesis of a key intermediate compound **7** which, when subjected to oxidative photocyclization in solution, provides precursor **2** that undergoes surface-catalyzed oxidative cyclization on Au(111) to yield the final product **1**. STM and STS characterization at sub-molecular level, in conjunction with a range of theoretical calculations, confirm the chemical structure of **1** and allow real-space visualization of the spin-split frontier orbitals. In particular, comparison of experimental STS data with GW+IC calculations suggests that **1** maintains its expected open-shell quartet ground state when adsorbed on Au(111). The high-spin, delocalized π-radical systems of π-extended triangulene and its homologues provide rich opportunities to conduct further studies on spin-spin interactions in pure hydrocarbon compounds and, as nanoscale organic ferromagnets, open perspectives toward applications in quantum electronic and spintronic devices.

ASSOCIATED CONTENT

Supporting Information

The Supporting Information is available free of charge on the ACS Publications website.
Detailed synthetic description of chemical compounds reported in this study (Scheme S1-S4) and associated solution characterization data (Fig. S5-S15), additional STM and STS data (Fig. S1-S3), additional calculations (Fig. S4), and experimental and calculation methods (PDF)

AUTHOR INFORMATION

Corresponding Author

*xinliang.feng@tu-dresden.de
*pascal.ruffieux@empa.ch

Author Contributions

⊥These authors contributed equally.

Notes

The authors declare no competing financial interests.

ACKNOWLEDGMENT

This work was supported by the Swiss National Science Foundation (grant numbers 200020-182015 and IZLCZ2-170184), the NCCR MARVEL funded by the Swiss National Science Foundation (grant number 51NF40-182892), the European Union's Horizon 2020 research and innovation program under grant agreement numbers 696656 and 785219 (Graphene Flagship Core 2), the Office of Naval Research (grant number N00014-18-1-2708), ERC Consolidator grant (T2DCP, number 819698), the German Research Foundation (DFG) within the Cluster of Excellence "Center for Advancing Electronics Dresden (cfaed)" and EnhanceNano (number 391979941), and the European Social Fund and the Federal State of Saxony (ESF-Project "GRAPHD", TU Dresden). Computational support from the Swiss Supercomputing Center (CSCS) under project ID s904 is gratefully acknowledged.

REFERENCES

(1) Narita, A.; Wang, X.-Y.; Feng, X.; Müllen, K. New Advances in Nanographene Chemistry. *Chem. Soc. Rev.* **2015**, *44* (18), 6616–6643.

(2) Nakada, K.; Fujita, M.; Dresselhaus, G.; Dresselhaus, M. S. Edge State in Graphene Ribbons: Nanometer Size Effect and Edge Shape Dependence. *Phys. Rev. B* **1996**, *54* (24), 17954–17961.

(3) *Physics and Chemistry of Graphene: Graphene to Nanographene*; Enoki, T., Ando, T., Eds.; Pan Stanford: Singapore, **2013**.

(4) Mishra, S.; Lohr, T. G.; Pignedoli, C. A.; Liu, J.; Berger, R.; Urgel, J. I.; Müllen, K.; Feng, X.; Ruffieux, P.; Fasel, R. Tailoring Bond Topologies in Open-Shell Graphene Nanostructures. *ACS Nano* **2018**, *12* (12), 11917–11927.

(5) Sun, Z.; Wu, J. Open-Shell Polycyclic Aromatic Hydrocarbons. *J. Mater. Chem.* **2012**, *22* (10), 4151–4160.

(6) Kubo, T.; Shimizu, A.; Sakamoto, M.; Uruichi, M.; Yakushi, K.; Nakano, M.; Shiomi, D.; Sato, K.; Takui, T.; Morita, Y.; Nakasuji, K. Synthesis, Intermolecular Interaction, and Semiconductive Behavior of a Delocalized Singlet Biradical Hydrocarbon. *Angew. Chem. Int. Ed.* **2005**, *44* (40), 6564–6568.

(7) Rudebusch, G. E.; Zafra, J. L.; Jorner, K.; Fukuda, K.; Marshall, J. L.; Arrechea-Marcos, I.; Espejo, G. L.; Ponce Ortiz, R.; Gómez-García, C. J.; Zakharov, L. N.; Nakano, M.; Ottosson, H.; Casado, J.; Haley, M. M. Diindeno-Fusion of an Anthracene as a Design Strategy for Stable Organic Biradicals. *Nat. Chem.* **2016**, *8* (8), 753–759.

(8) Nakano, M.; Champagne, B. Nonlinear Optical Properties in Open-Shell Molecular Systems. *Wiley Interdiscip. Rev. Comput. Mol. Sci.* **2016**, *6* (2), 198–210.

(9) Smith, M. B.; Michl, J. Singlet Fission. *Chem. Rev.* **2010**, *110* (11), 6891–6936.

(10) Yazyev, O. V. Emergence of Magnetism in Graphene Materials and Nanostructures. *Rep. Prog. Phys.* **2010**, *73* (5), 056501.

(11) Bullard, Z.; Girão, E. C.; Owens, J. R.; Shelton, W. A.; Meunier, V. Improved All-Carbon Spintronic Device Design. *Sci. Rep.* **2015**, *5*, 7634.

(12) Morita, Y.; Suzuki, S.; Sato, K.; Takui, T. Synthetic Organic Spin Chemistry for Structurally Well-Defined Open-Shell Graphene Fragments. *Nat. Chem.* **2011**, *3* (3), 197–204.

(13) Randić, M. Aromaticity of Polycyclic Conjugated Hydrocarbons. *Chem. Rev.* **2003**, *103* (9), 3449–3606.

(14) Wang, W. L.; Yazyev, O. V.; Meng, S.; Kaxiras, E. Topological Frustration in Graphene Nanoflakes: Magnetic Order and Spin Logic Devices. *Phys. Rev. Lett.* **2009**, *102* (15), 157201.

(15) Bullard, Z.; Costa Girão, E.; Daniels, C.; Sumpter, B. G.; Meunier, V. Quantifying Energetics of Topological Frustration in Carbon Nanostructures. *Phys. Rev. B* **2014**, *89* (24), 245425.

(16) Ovchinnikov, A. A. Multiplicity of the Ground State of Large Alternant Organic Molecules with Conjugated Bonds. *Theor. Chim. Acta* **1978**, *47* (4), 297–304.

(17) Goto, K.; Kubo, T.; Yamamoto, K.; Nakasuji, K.; Sato, K.; Shiomi, D.; Takui, T.; Kubota, M.; Kobayashi, T.; Yakusi, K.; Ouyang, J. A Stable Neutral Hydrocarbon Radical: Synthesis, Crystal Structure, and Physical Properties of 2,5,8-Tri-*tert*-butylphenalenyl. *J. Am. Chem. Soc.* **1999**, *121* (7), 1619–1620.

(18) Allinson, G.; Bushby, R. J.; Paillaud, J. L.; Oduwole, D.; Sales, K. ESR Spectrum of a Stable Triplet π Biradical: Trioxytriangulene. *J. Am. Chem. Soc.* **1993**, *115* (5), 2062–2064.

(19) Allinson, G.; Bushby, R. J.; Jesudason, M. V.; Paillaud, J.-L.; Taylor, N. The Synthesis of Singlet Ground State Derivatives of Non-Kekulé Polynuclear Aromatics. *J. Chem. Soc. Perkin Trans. 2* **1997**, *0* (2), 147–156.

(20) Inoue, J.; Fukui, K.; Kubo, T.; Nakazawa, S.; Sato, K.; Shiomi, D.; Morita, Y.; Yamamoto, K.; Takui, T.; Nakasuji, K. The First Detection of a Clar's Hydrocarbon, 2,6,10-Tri-*tert*-Butyltriangulene: A Ground-State Triplet of Non-Kekulé Polynuclear Benzenoid Hydrocarbon. *J. Am. Chem. Soc.* **2001**, *123* (50), 12702–12703.

(21) Pavliček, N.; Mistry, A.; Majzik, Z.; Moll, N.; Meyer, G.; Fox, D. J.; Gross, L. Synthesis and Characterization of Triangulene. *Nat. Nanotechnol.* **2017**, *12* (4), 308–311.

(22) Clar, E.; Stewart, D. G. Aromatic Hydrocarbons. LXV. Triangulene Derivatives[1]. *J. Am. Chem. Soc.* **1953**, *75* (11), 2667–2672.
(23) *On-Surface Synthesis*; Gourdon, A., Ed.; Springer International Publishing: Cham, **2016**.
(24) Barbasiewicz, M.; Michalak, M.; Grela, K. A New Family of Halogen-Chelated Hoveyda–Grubbs-Type Metathesis Catalysts. *Chem. – Eur. J.* **2012**, *18* (45), 14237–14241.
(25) Takesue, T.; Fujita, M.; Sugimura, T.; Akutsu, H. A Series of Two Oxidation Reactions of Ortho-Alkenylbenzamide with Hypervalent Iodine(III): A Concise Entry into (3*R*,4*R*)-4-Hydroxymellein and (3*R*,4*R*)-4-Hydroxy-6-methoxymellein. *Org. Lett.* **2014**, *16* (17), 4634–4637.
(26) Zhang, Y.-B.; Furukawa, H.; Ko, N.; Nie, W.; Park, H. J.; Okajima, S.; Cordova, K. E.; Deng, H.; Kim, J.; Yaghi, O. M. Introduction of Functionality, Selection of Topology, and Enhancement of Gas Adsorption in Multivariate Metal–Organic Framework-177. *J. Am. Chem. Soc.* **2015**, *137* (7), 2641–2650.
(27) Gross, L.; Mohn, F.; Moll, N.; Liljeroth, P.; Meyer, G. The Chemical Structure of a Molecule Resolved by Atomic Force Microscopy. *Science* **2009**, *325* (5944), 1110–1114.
(28) Gross, L.; Mohn, F.; Moll, N.; Meyer, G.; Ebel, R.; Abdel-Mageed, W. M.; Jaspars, M. Organic Structure Determination Using Atomic-Resolution Scanning Probe Microscopy. *Nat. Chem.* **2010**, *2* (10), 821–825.
(29) Kichin, G.; Weiss, C.; Wagner, C.; Tautz, F. S.; Temirov, R. Single Molecule and Single Atom Sensors for Atomic Resolution Imaging of Chemically Complex Surfaces. *J. Am. Chem. Soc.* **2011**, *133* (42), 16847–16851.
(30) Das, A.; Müller, T.; Plasser, F.; Lischka, H. Polyradical Character of Triangular Non-Kekulé Structures, Zethrenes, p-Quinodimethane-Linked Bisphenalenyl, and the Clar Goblet in Comparison: An Extended Multireference Study. *J. Phys. Chem. A* **2016**, *120* (9), 1625–1636.

Table of Contents artwork